0 0 0 0 4 9 0 3 5 8 4

Submitted to Journal of Applied Physics

UC-25

LBL-6990
Preprint

c.1

EROSION PREDICTION NEAR A STAGNATION POINT RESULTING FROM ENVIRONMENTAL SOLID PARTICLES

RECEIVED
LAWRENCE
BERKELEY LABORATORY

MAY 24 1978

LIBRARY AND
DOCUMENTS SECTION

J. Laitone

November 1977

Prepared for the U. S. Department of Energy
under Contract W-7405-ENG-48

For Reference

Not to be taken from this room

LAWRENCE BERKELEY LABORATORY
UNIVERSITY OF CALIFORNIA
25

LBL-6990
c.1

LEGAL NOTICE

This report was prepared as an account of work sponsored by the United States Government. Neither the United States nor the Department of Energy, nor any of their employees, nor any of their contractors, subcontractors, or their employees, makes any warranty, express or implied, or assumes any legal liability or responsibility for the accuracy, completeness or usefulness of any information, apparatus, product or process disclosed, or represents that its use would not infringe privately owned rights.

0 0 0 0 4 9 0 3 3 8 5

LBL 6990

EROSION PREDICTION NEAR A STAGNATION POINT RESULTING FROM ENVIRONMENTAL SOLID PARTICLES

J. Laitone

Materials and Molecular Research Division
Lawrence Berkeley Laboratory
University of California
Berkeley, California 94720

0 0 0 0 4 9 0 3 5 8 6

ABSTRACT

Predicting the erosion that results from a gas-solid particle flow in coal energy conversion systems is crucial for the successful operation of coal gasification, magnetohydrodynamic power, and coal-fired turbine facilities. In this study the coupled gas-particle momentum equations are analytically solved to determine the particle trajectories near a plane stagnation point. The momentum equilibration parameter, which is a physical parameter measuring a particle's momentum, is found to be the unique criterion for predicting particle trajectories. It is shown that values of this parameter less than one-fourth identify particles that never impact with a wall. The closed-form solution obtained is used to predict the quantity of material removed from a wall as well as the location of erosion along the wall. The maximum erosion is calculated to occur for the momentum equilibration parameter taking a value of 2.3. The erosion rate is found to be proportional to the particle velocity raised to the exponent of 3.8 .

LIST OF SYMBOLS

E = relative erosion rate

J_o = particle number flux at wall

$\dot{M}$ = particle mass flux

$N_{p\infty}$ = particle number density, free stream

q = particle impact speed

t = time

U = fluid velocity, free stream

$\vec{v}_p$ = particle velocity

$\vec{v}$ = fluid velocity

W = complex potential

X = characteristic length x direction ($x = X$ when $u = u_p = U$)

Y = characteristic length y direction ($y = Y$ when $v = v_p = V$)

Y_o = particle impact coordinate

z = nondimensional time

z_s = nondimensional time when particle impacts

α = relative angle between particle path and wall surface

β = particle initial y/Y - coordinate

γ = scaling factor $\gamma = X/Y$

σ = particle radius

ρ_s = mass of particle per unit volume of particle material

τ = momentum equilibration time

λ_m' = momentum equilibration length (nondimensional)

0 0 0 0 4 9 0 3 5 8 7

1. INTRODUCTION

For many years gas-solid particle flows have interested scientists and engineers. Gas-particle flow phenomena are important in sedimentation pipe flows, fluidized beds, and transport processes. More recently the fields of propulsion, combustion, and energy conversion have stimulated new interest in this area of two-phase flow.

In particular, magnetohydrodynamic coal energy conversion, geothermal conversion, and coal gasification are three areas where a thorough understanding of gas-solid flows and the subsequent erosion is crucial.

This study treats the problem of determining the particle trajectories and resulting erosion near a stagnation point. This is a critical area arising in a corner flow, flow into a flat plate, and flows over closed bodies such as cylinders and blades. The study endeavors to identify the primary factors that determine erosion behavior.

As a specific example the gas-particle flow typical of a coal gasification system is analyzed.

2. EQUATIONS OF MOTION

The equations of motion of a particle in a steady stream with velocity components u,v have been derived[1] and are presented here in the following form:

$$\frac{Du_p}{Dt} = \frac{u-u_p}{\tau} , \tag{1}$$

$$\frac{Dv_p}{Dt} = \frac{v-v_p}{\tau} , \tag{2}$$

where $\tau = \frac{2}{9} \frac{\rho_s \sigma^2}{\mu}$.

It is assumed that the dispersed particle phase is sufficiently dilute so that the mixture behaves as if it were made up of the continuous phase alone. Therefore, the particles do not significantly affect the continuous phase. Furthermore, the particle Reynolds number is assumed to be of order unity. Thus the volume force acting on the particle has the form of the Stoke's drag law. A detailed order of magnitude analysis that considers the preceding and following assumptions is available.[2]

Other assumptions are:

1) The particles are spherical and all of constant size.
2) Pressure, lift, gravitational, and viscous forces are negligible.
3) Brownian motion is negligible.
4) The continuous phase is incompressible.

Since $u_p = \frac{Dx}{Dt}$ and $v_p = \frac{Dy}{Dt}$, substitution into Eqs. (1) and (2) yields

$$\tau \frac{d^2x}{dt^2} + \frac{dx}{dt} - u = 0 , \tag{3}$$

$$\tau \frac{d^2y}{dt^2} + \frac{dy}{dt} - v = 0 \ . \tag{4}$$

Now consider the inviscid flow near the stagnation point. The complex potential is given outside the thin boundary layer as:

$$W = - \tfrac{1}{2} \frac{U}{X} z^2 \ ,$$

where X is some distance ahead of the stagnation point where free stream conditions exist $(u = - U)$. The velocity components corresponding to this flow are

$$u = - \frac{U}{X} x \ , \tag{5}$$

$$v = \frac{U}{X} y \ . \tag{6}$$

Make a change of variables; let

$$z = t/\tau, \ \lambda'_m = \frac{\tau U}{X} = \frac{\lambda_m}{X} \ ,$$

where λ'_m is the momentum equilibration length parameter (frequently referred to as the inertia parameter). Physically, λ_m is a number that indicates the distance required for a particle to travel in order to reduce its initial slip velocity by e^{-1} . Likewise, τ is referred to as the momentum equilibration time.

Equations (3) and (4) with (5) and (6) become

$$\frac{d^2x}{dz^2} + \frac{dx}{dz} + \lambda'_m x = 0 \ , \tag{7}$$

$$\frac{d^2y}{dz^2} + \frac{dy}{dz} - \lambda'_m y = 0 \ . \tag{8}$$

A. Solution procedure

Equation (8) has solution

$$y = A_1 \, e^{r_1 z} + A_2 \, e^{r_2 z} \quad , \tag{9}$$

$$r_1 = -\tfrac{1}{2} + \tfrac{1}{2}\,(1+4\lambda'_m)^{\frac{1}{2}}, r_2 = -\tfrac{1}{2} - \tfrac{1}{2}\,(1+4\lambda'_m)^{\frac{1}{2}} \quad . \tag{10}$$

Equation (7) has solutions of different form depending on the value of λ'_m .

<u>Case $\lambda'_m < \frac{1}{4}$</u>

Here

$$x = A_3 \, e^{r_3 z} + A_4 \, e^{r_4 z} \quad , \tag{11}$$

$$r_3 = -\tfrac{1}{2} + \tfrac{1}{2}\,(1-4\lambda'_m)^{\frac{1}{2}} \; , \; r_4 = -\tfrac{1}{2} - \tfrac{1}{2}\,(1-4\lambda'_m)^{\frac{1}{2}} \quad . \tag{12}$$

To solve for A_2 and A_3 , assume an initial condition that at the plane $x = X$ the particles have the gas stream velocity

$$u_p = -U = \frac{dx}{dt} = \frac{1}{\tau}\frac{dx}{dz} \quad . \tag{13}$$

Now if $t = 0$ $(z = 0)$ when $x = X$, then from (11) $X = A_3 + A_4$ and Eq. (13) gives: $(r_3+\lambda_m)\,A_3 + (r_4+\lambda_m)\,A_4 = 0$.

Thus

$$\frac{x}{X} = \left(\frac{r_4+\lambda'_m}{r_4-r_3}\right) e^{r_3 z} + \left(\frac{r_3+\lambda'_m}{r_3-r_4}\right) e^{r_4 z} \quad . \tag{14}$$

The particles that are at some initial position X traveling with the gas will hit the plate, provided that $x = 0$ for some finite z_s . Otherwise the particles will only approach the plate asymptotically.

Thus

$$0 = \left(\frac{r_4+\lambda'_m}{r_4-r_3}\right) e^{r_3 z_s} + \left(\frac{r_3+\lambda'_m}{r_3-r_4}\right) e^{r_4 z_s}$$

$$\therefore z_s = \frac{1}{r_3-r_4} \ln \left(\frac{r_3+\lambda'_m}{r_4+\lambda'_m}\right)$$

Now $r_3-r_4 = (1-4\lambda'_m)^{\frac{1}{2}} > 0$ since $0 \leqslant \lambda_m < \frac{1}{4}$. Similarly,

$$r_3 + \lambda'_m < 0 \qquad\qquad - \tfrac{1}{2} < r_3+\lambda'_m < 0$$

and

$$r_4 + \lambda'_m < 0 \qquad\qquad - 1 < r_4+\lambda'_m < - \tfrac{1}{4}$$

$$\therefore + \tfrac{1}{2} < r_4+\lambda'_m < r_3+\lambda'_m < 0 .$$

Thus, $z_s < 0$ and at no time will the particles strike the plate.

<u>Case $\lambda'_m > \frac{1}{4}$</u>

Here

$$x = A'_5 \, e^{[-\frac{1}{2}+i\frac{1}{2}(4\lambda'_m-1)^{\frac{1}{2}}]z} + A'_6 \, e^{[-\frac{1}{2}-i\frac{1}{2}\,(4\lambda'_m-1)^{\frac{1}{2}}]z},$$

$$= A_5 \, e^{-\frac{1}{2}z} \cos(\lambda'_m-\tfrac{1}{4})^{\frac{1}{2}} z + A_6 \, e^{-\frac{1}{2}z} \sin(\lambda'_m-\tfrac{1}{4})^{\frac{1}{2}} z . \qquad (15)$$

Assume an initial condition at $t = 0$ ($z = 0$)

$x = X$

and $u_p = \frac{dx}{dt} = - U = \frac{1}{\tau}\frac{dx}{dz}$

Then Eq. (15) gives $A_5 = X$

and $-\lambda'_m X = A_6 \, (\lambda'_m-\tfrac{1}{4})^{\frac{1}{2}} - \tfrac{1}{2}A_5$

$$\therefore A_6 = \left[\frac{-\lambda'_m + \frac{1}{2}}{(\lambda'_m-\frac{1}{4})^{\frac{1}{2}}}\right] X .$$

Thus

$$\frac{x}{X} = e^{-\frac{1}{2}z} \left[\cos\ (\lambda'_m - \tfrac{1}{4})^{\frac{1}{2}} z + \frac{\frac{1}{2} - \lambda'_m}{(\lambda'_m - \frac{1}{4})^{\frac{1}{2}}} \sin\ (\lambda'_m - \tfrac{1}{4})^{\frac{1}{2}} z \right] \quad . \tag{16}$$

When $x = 0$

$$0 = \cos\ (\lambda'_m - \tfrac{1}{4})^{\frac{1}{2}} z_s + \frac{\frac{1}{2} - \lambda'_m}{(\lambda'_m - \frac{1}{4})^{\frac{1}{2}}} \sin\ (\lambda'_m - \tfrac{1}{4})^{\frac{1}{2}} z_s \tag{17}$$

$$\therefore \tan\ (\lambda'_m - \tfrac{1}{4})^{\frac{1}{2}} z_s = \frac{(\lambda'_m - \frac{1}{4})^{\frac{1}{2}}}{(\lambda'_m - \frac{1}{2})} \quad . \tag{18}$$

As z_s decreases from π to $\frac{\pi}{2}$, λ'_m increases from $\frac{1}{4}$ to $\frac{1}{2}$.

As λ'_m increases from $\frac{1}{2}$ to ∞, z_s decreases from π to 0.

Thus if $\lambda'_m > \frac{1}{4}$ the particles will always strike the plane, provided they are at some $x = X$ moving with the gas.

Case $\lambda'_m = \frac{1}{4}$

Here

$$x = A_7\ e^{-\frac{1}{2}z} + A_8\ z\ e^{-\frac{1}{2}z} \quad . \tag{19}$$

Assume an initial condition at $t = 0$.

$(z = 0)$ $x = X$ and

$u_p = \frac{dx}{dt} = -\ U = \frac{1}{\tau}\frac{dx}{dz}$.

Then Eq. (19) gives $A_7 = X$

and

$-\ \lambda'_m X = -\ \frac{1}{2}X\ e^{-\frac{1}{2}z} - \frac{1}{2}A_8 z\ e^{-\frac{1}{2}z} + A_8\ e^{-\frac{1}{2}z}$.

So that

$$A_8 = \tfrac{1}{2}X - \lambda'_m X = \tfrac{1}{4}X \ .$$

Then

$$\frac{x}{X} = e^{-\frac{1}{2}z} + \tfrac{1}{4}z\ e^{-\frac{1}{2}z}$$

$$= e^{-\frac{1}{2}z}\ (1 + \tfrac{1}{4}z) \quad . \tag{20}$$

The solution to Eq. (9) gives the y path.

Assume the initial condition $y = Y$ when $x = X$ at $z = 0$. Then, from Eq. (9)

$$Y = A_1 + A_2 \ . \tag{21}$$

For the second condition we consider two cases:

<u>Case A) $v_p = 0$</u>

Then

$$0 = A_1 r_1 + A_2 r_2$$

and

$$0 = Y r_1 - A_2 r_1 + A_2 r_2 \ .$$

Thus

$$A_2 = Y\ r_1/(r_1 - r_2)$$

$$A_1 = Y\left(\frac{-r_2}{r_1 - r_2}\right) \quad .$$

Thus

$$\frac{y}{Y} = (-r_2\ e^{r_1 z} + r_1\ e^{r_2 z})\ /\ r_1 - r_2 \tag{22}$$

$$\therefore\ \frac{y}{Y} = \left[\left\{\tfrac{1}{2}+\tfrac{1}{2}(1+4\lambda'_m)^{\frac{1}{2}}\right\} e^{\left[-\frac{1}{2}+\frac{1}{2}(1+4\lambda'_m)^{\frac{1}{2}}\right]z}\right.$$

$$\left. + \left\{-\tfrac{1}{2}+\tfrac{1}{2}(1+4\lambda'_m)^{\frac{1}{2}}\right\} e^{\left[-\frac{1}{2}-\frac{1}{2}(1+4\lambda'_m)^{\frac{1}{2}}\right]z}\right]\ /\ (1+4\lambda'_m)^{\frac{1}{2}} \ . \tag{23}$$

See Fig. 1.

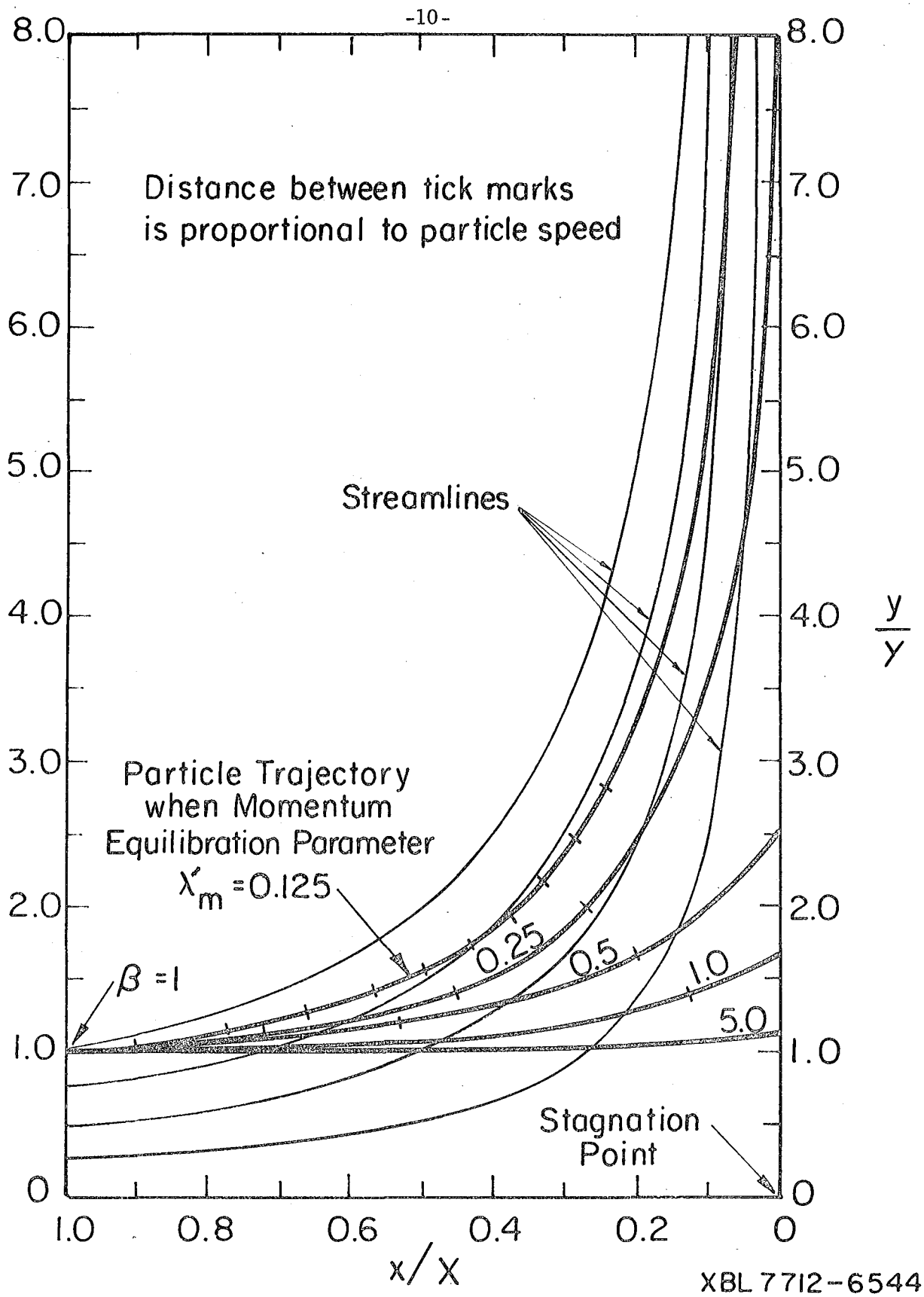

FIG. 1. Particle trajectories. The momentum equilibration parameter indicates the magnitude of a particle's momentum. When $\lambda'_m > 10$ the trajectories are almost entirely determined by initial conditions. For $\lambda'_m \leqslant 0.25$, the particles are completely entrained in the gas flow and never impact with the wall.

Case B) The particles follow the stream line.

Initially $v_p = v = \frac{UY}{X} = \frac{dy}{dt} = \frac{1}{\tau}\frac{dy}{dz}$.

Then

$$\lambda'_m Y = A_1 r_1 + A_2 r_2 \ .$$

Combining this with Eq. (21) we obtain

$$0 = (r_1 - \lambda'_m)\ A_1 + (r_2 - \lambda'_m)\ A_2 \ .$$

Then

$$0 = (r_1 - \lambda'_m)\ A_1 + (r_2 - \lambda'_m)\ Y - (r_2 - \lambda'_m)\ A_1 \ ,$$

so that

$$A_1\ (r_1 - r_2) = (\lambda'_m - r_2)\ Y \ .$$

Hence

$$A_1 = Y \frac{(\lambda'_m - r_2)}{(r_1 - r_2)}$$

$$A_2 = Y \left(1 - \frac{\lambda'_m - r_2}{r_1 - r_2}\right)$$

$$= Y \frac{r_1 - \lambda'_m}{r_1 - r_2} \ .$$

The y trajectories are therefore given by

$$\frac{y}{Y} = \left(\frac{\lambda'_m - r_2}{r_1 - r_2}\right) e^{r_1 z} + \left(\frac{r_1 - \lambda'_m}{r_1 - r_2}\right) e^{r_2 z} \ . \qquad (24)$$

3. RESULTS AND DISCUSSIONS

A. Method of determining impact density, speed, and angle

As the momentum equilibration time τ increases (i.e., as λ'_m increases), $z \to 0$. In the limit $\tau \to \infty$, if Yo is the y value for the particle striking the plane $x = 0$, we find that in case A) $Yo/Y \to 1$, and in case B) $Yo/Y \to 1$.

From Eqs. (23) and (24) we see that Yo/Y is a function of λ'_m only. Thus the number density of particles along the wall $(x = 0)$ is constant for a given λ'_m. Since all particles for which $y/Y < 1$ will strike the plane at a distance less than Y_o, we arrive at the result

$$\frac{Yo}{Y} = \frac{\text{Number of particles crossing unit area when moving with fluid per unit time}}{\text{Number of particles striking unit area at } x = 0 \text{ per unit time}} .$$

Thus if $N_{p\infty} = \dfrac{\text{Number of particles in free stream}}{\text{unit volume}}$,

U = Free stream gas velocity

$$J_o = \frac{\text{Number of particles striking wall}}{\text{unit area unit time}} .$$

Then

$$J_o = \frac{Y}{Y_o} N_{p\infty} U = \frac{Y}{Y_o} J_{o\infty} . \tag{25}$$

The variation of J_o/J_∞ with λ_m/X is shown in Fig. 2. For particles for which initially $y/Y = \beta$ $(0 \leqslant \beta \leqslant 1)$ and $\lambda'_m > \frac{1}{4}$ the trajectories in case A are given by

$$\frac{x}{X}\Big|_{\beta=\beta} = e^{-\frac{1}{2}z} \left\{ \cos\left(\lambda'_m - \tfrac{1}{4}\right)^{\frac{1}{2}} z + \left[\frac{\frac{1}{2} - \lambda'_m}{\left(\lambda'_m - \frac{1}{4}\right)^{\frac{1}{2}}}\right] \sin\left(\lambda'_m - \tfrac{1}{4}\right)^{\frac{1}{2}} z \right\} = \frac{x}{X}\Big|_{\beta=1} \tag{26}$$

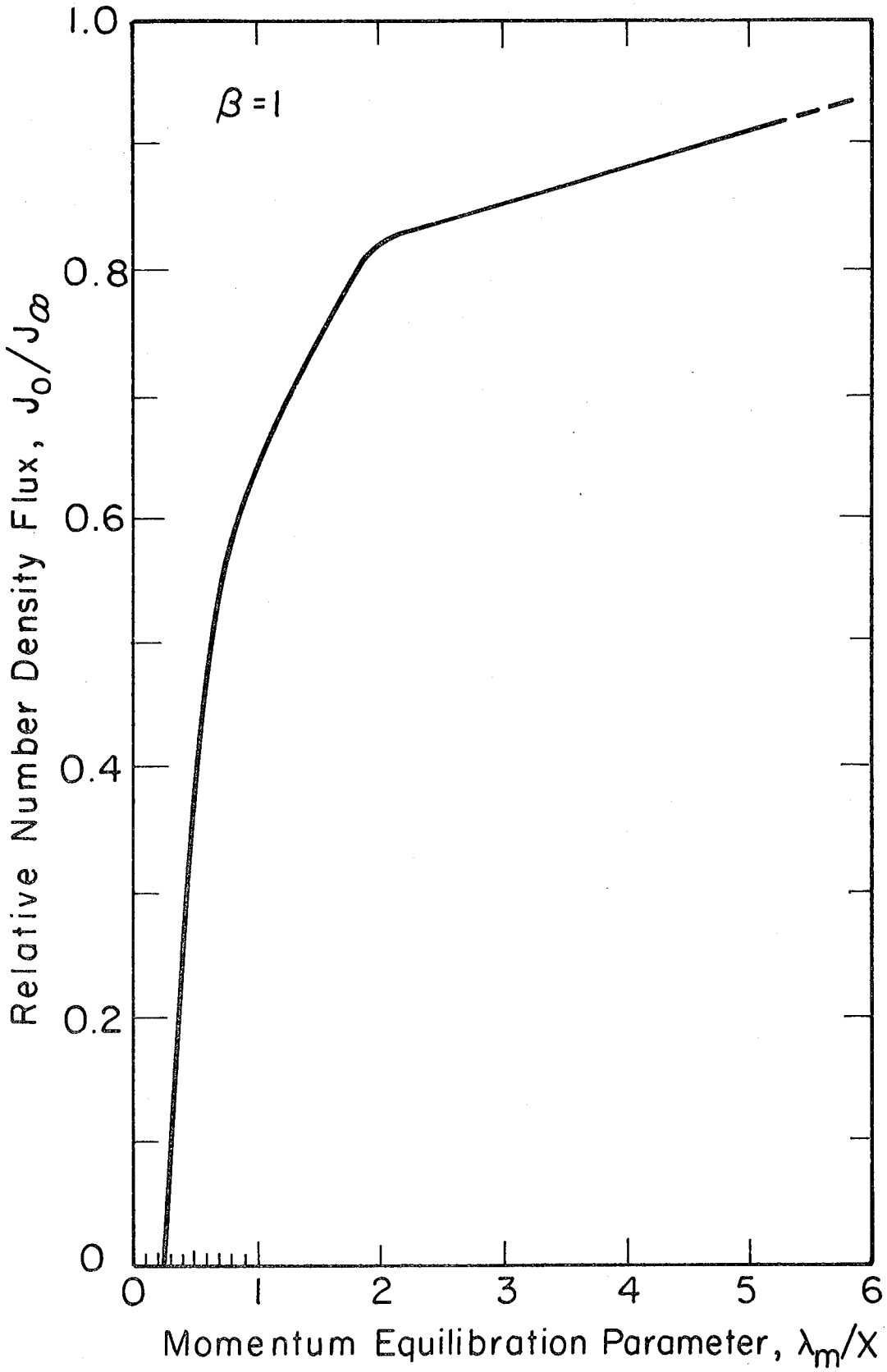

FIG. 2. Relative number density flux as a function of the momentum euqilibration parameter. Particles with high momentum will impact with a number density approaching that found in the free stream region ($J_0/J_\infty \to 1$).

XBL7712-6545

$$\frac{y}{Y}\Big|_{\beta=\beta} = \beta \left\{ \left[\tfrac{1}{2}+\tfrac{1}{2}\,(1+4\lambda'_m)^{\frac{1}{2}}\right] e^{\left[-\frac{1}{2}+\frac{1}{2}(1+4\lambda'_m)^{\frac{1}{2}}\right]z} + \left[-\tfrac{1}{2}+\tfrac{1}{2}(1+4\lambda'_m)^{\frac{1}{2}}\right] e^{\left[-\frac{1}{2}-\frac{1}{2}(1+4\lambda'_m)^{\frac{1}{2}}\right]z} \right\} \Big/ (1+4\lambda'_m)^{\frac{1}{2}}$$

$$= \beta \frac{y}{Y}\Big|_{\beta=1} . \tag{27}$$

Furthermore the speed on impact q (letting $\gamma = X/Y$) is given by (see Fig. 3)

$$\frac{q}{U} = \frac{1}{\lambda'_m} \left\{ \left[\frac{1}{X}\frac{dx}{dz}\Big|_{z=z_s}\right]^2 + \frac{\beta^2}{\gamma^2}\left[\frac{1}{Y}\frac{dy}{dz}\Big|_{z=z_s}\right]^2 \right\}^{\frac{1}{2}} , \tag{28}$$

where z_s is given in Eq. (18).

When $x = 0$, $z = z_s$ and $y = Y_o$, and

$$\frac{1}{X}\frac{dx}{dz} = e^{-\frac{1}{2}z} \left\{ \frac{\frac{3}{4} - 2\lambda'_m}{(\lambda'_m - \frac{1}{4})^{\frac{1}{2}}} \sin(\lambda'_m - \tfrac{1}{4})^{\frac{1}{2}} z - \lambda'_m \cos(\lambda'_m - \tfrac{1}{4})^{\frac{1}{2}} z \right\} ,$$

$$\frac{1}{Y}\frac{dy}{dz} = \frac{r_1 r_2}{r_1 - r_2} \left\{ e^{r_2 z} - e^{r_1 z} \right\} .$$

The angle of impact is (see Fig. 4)

$$\alpha = \tan^{-1} \left\{ \frac{\gamma \frac{1}{X}\frac{dx}{dz}\Big|_{z=z_s}}{\beta \frac{1}{Y}\frac{dy}{dz}\Big|_{z=z_s}} \right\} \tag{29}$$

where α is measured from the wall to the particle trajectory.

By assigning successive values to β over the interval $0 < y/Y \leqslant 1$ and solving for a fixed λ'_m , the particle trajectories Eqs. (26) and (27), the impact speed Eq. (28), and the impact angle Eq. (29) are obtained for a distribution of similar particles. Since the particles are all of the same size and density, for a given distribution no particle-particle collision will occur before impact with the wall. However, this model does not take into account particles that rebound from the wall.

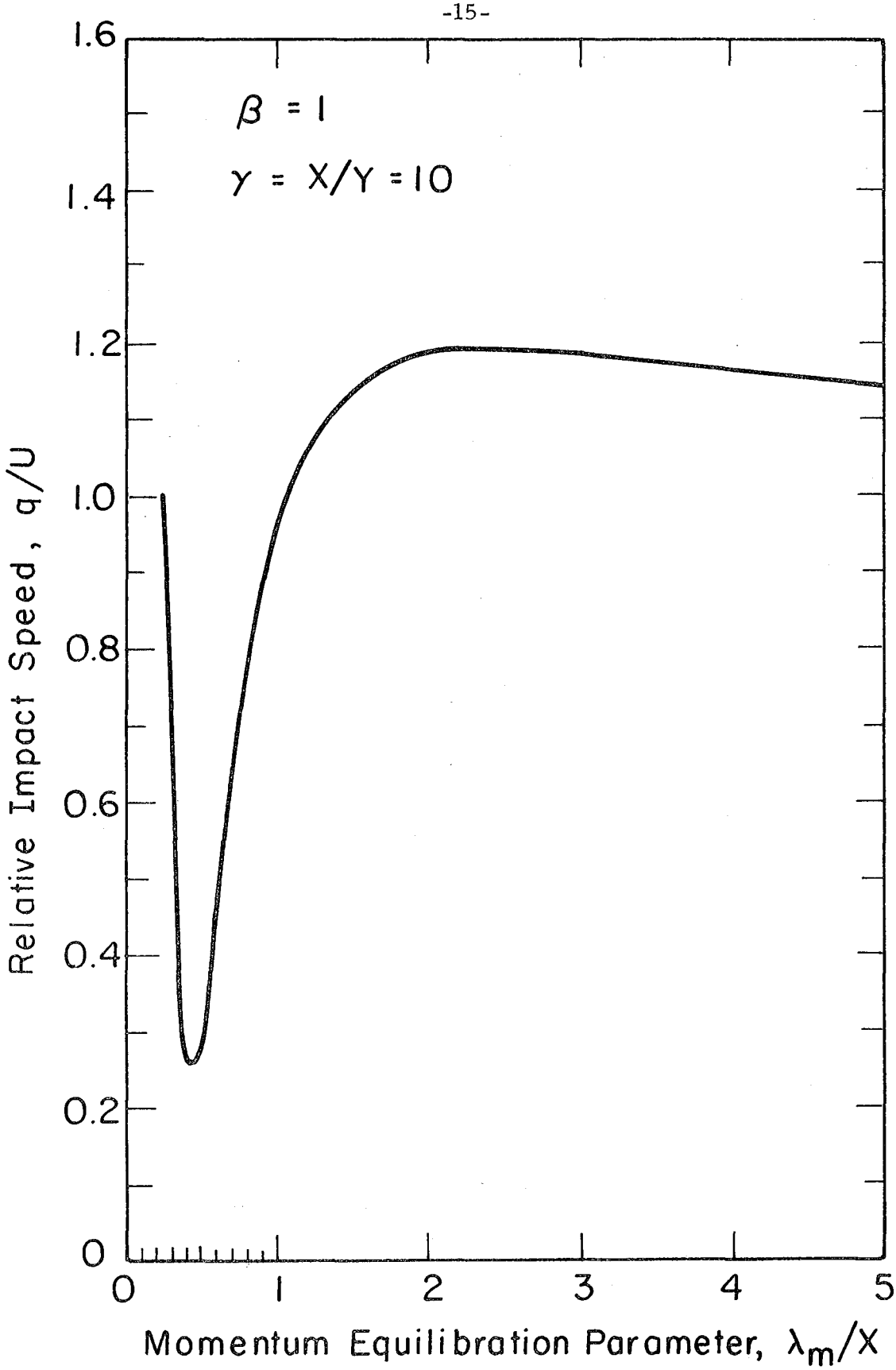

FIG. 3. Relative particle impact speed as a function of the momentum equilibration parameter. The increase in particle impact speed for $0.25 < \lambda'_m < 0.40$ is due to the gas accelerating the particle away from the stagnation point.

XBL7712-6546

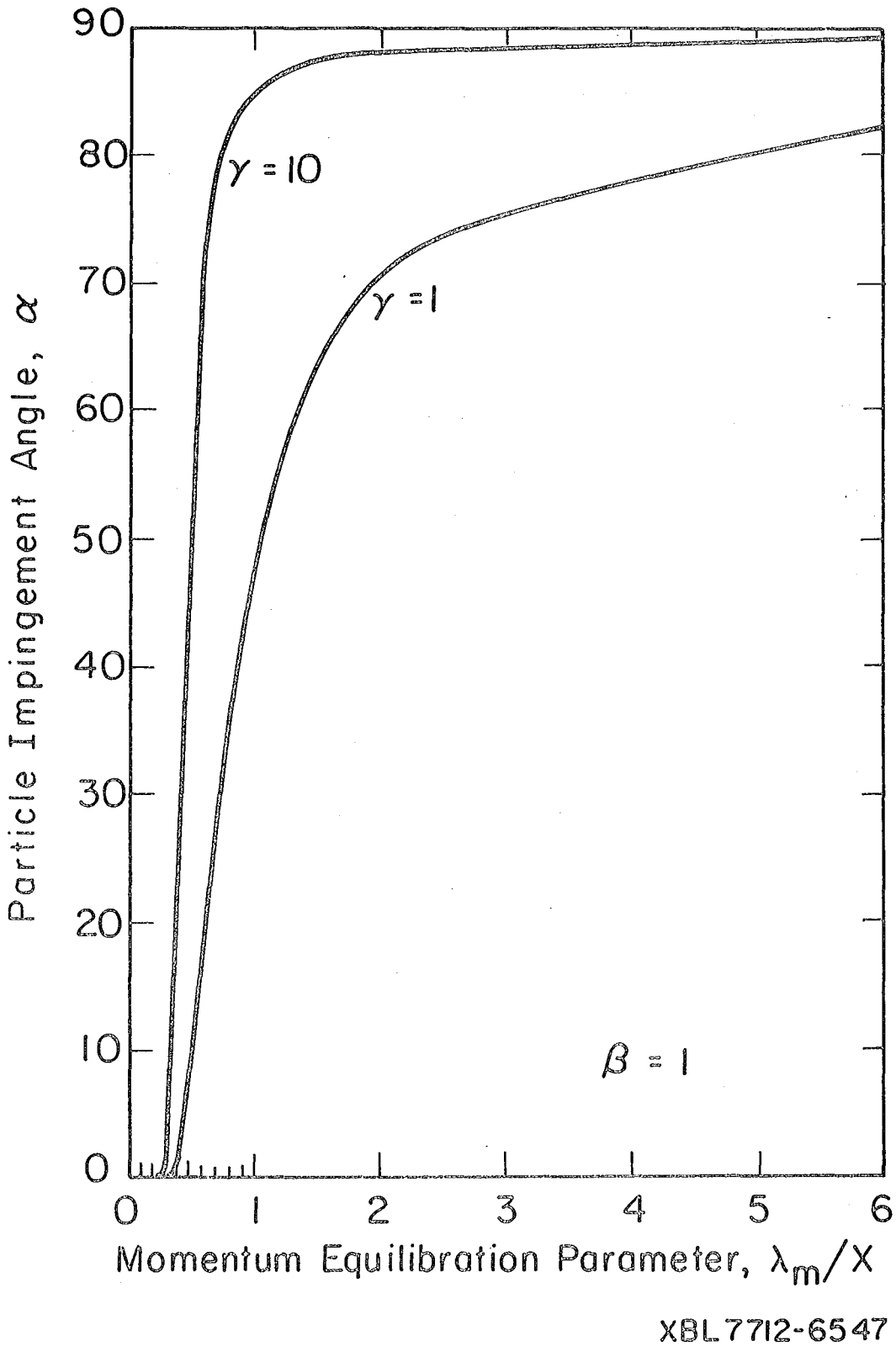

FIG. 4. Particle impingement angle as a function of momentum equilibration parameter. The initial position of a particle is given by $\gamma = X/Y$.

Rebounding particles may collide with approaching particles, leading to multiple impacts at the wall. The rebound angles and coefficient of restitution depend on particle size, impact angle and velocity.[3] Thus a complete description of the resulting erosion would appear to require a statistical model of particle-particle interaction and particle-wall rebound, which is outside the scope of this work.

B. Erosion distribution on the wall

The relative erosion can now be calculated using the following expression developed by Finnie.[4]

$$E = \frac{\dot{M}\, q^2\, F(\alpha)}{\dot{M}_{max}\, q^2_{max}} ,$$

where

E = relative magnitude of erosion rate,

$\dot{M}$ = mass flux of eroding particles,

q = particle speed at impact,

$F(\alpha)$ = scaling function (nondimensional) based on predicted and observed values of erosion of a ductile material by particles impinging at varying angles (see Fig. 6).

The model on which this expression is based assumes that the particles act as cutting tools, with the cutting depth a function of the hardness of the surface material. No account is taken in the model of particle size effects for particles less than about 100μm. For particles larger than 100μm erosion is independent of size. However, for small particles erosion becomes less efficient with decreasing particle size.[5]

In this study the size effect is also neglected since the particle is characterized by the momentum equilibration parameter, which is

multiple valued (i.e., a large particle with low velocity can have the same value of λ'_m as a small particle with a high velocity). The dimensional cases investigated in this study are based on erosion results from particles larger than 100μm.

Rewriting, the relative erosion rate is:

$$E = \frac{(J_o \frac{4}{3}\pi\sigma^3 \rho_s \quad q)\ q^2\ F(\alpha)}{(J_{o_{max}} \frac{4}{3}\pi\sigma^3 \rho_s \quad q_{max})\ q^2_{max}}$$

$$= \frac{J_o\ q^3\ F(\alpha)}{J_{o_{max}}\ q^3_{max}} \quad . \tag{30}$$

The relative erosion is plotted in Fig. 5 as a function of the momentum equilibration parameter. The shape of the curve is clearly dictated by the impact speed variations since the erosion varies with the cube of the speed.

C. Effect of particle velocity

The intriguing shape of the erosion curve shown in Fig. 6 can be explained by examining the velocity components of the particles. As is expected, particles with large λ'_m are relatively unaffected by the continuous phase, and travel in straight lines with trajectories determined by the initial conditions. As λ'_m decreases to a value of 2, the particles experience a very slight deceleration through the continuous phase in the x direction, along with an acceleration in the y direction due to the continuous phase accelerating away from the stagnation point. The overall increase in speed and erosion then is due to the magnitude of the vector sum of these

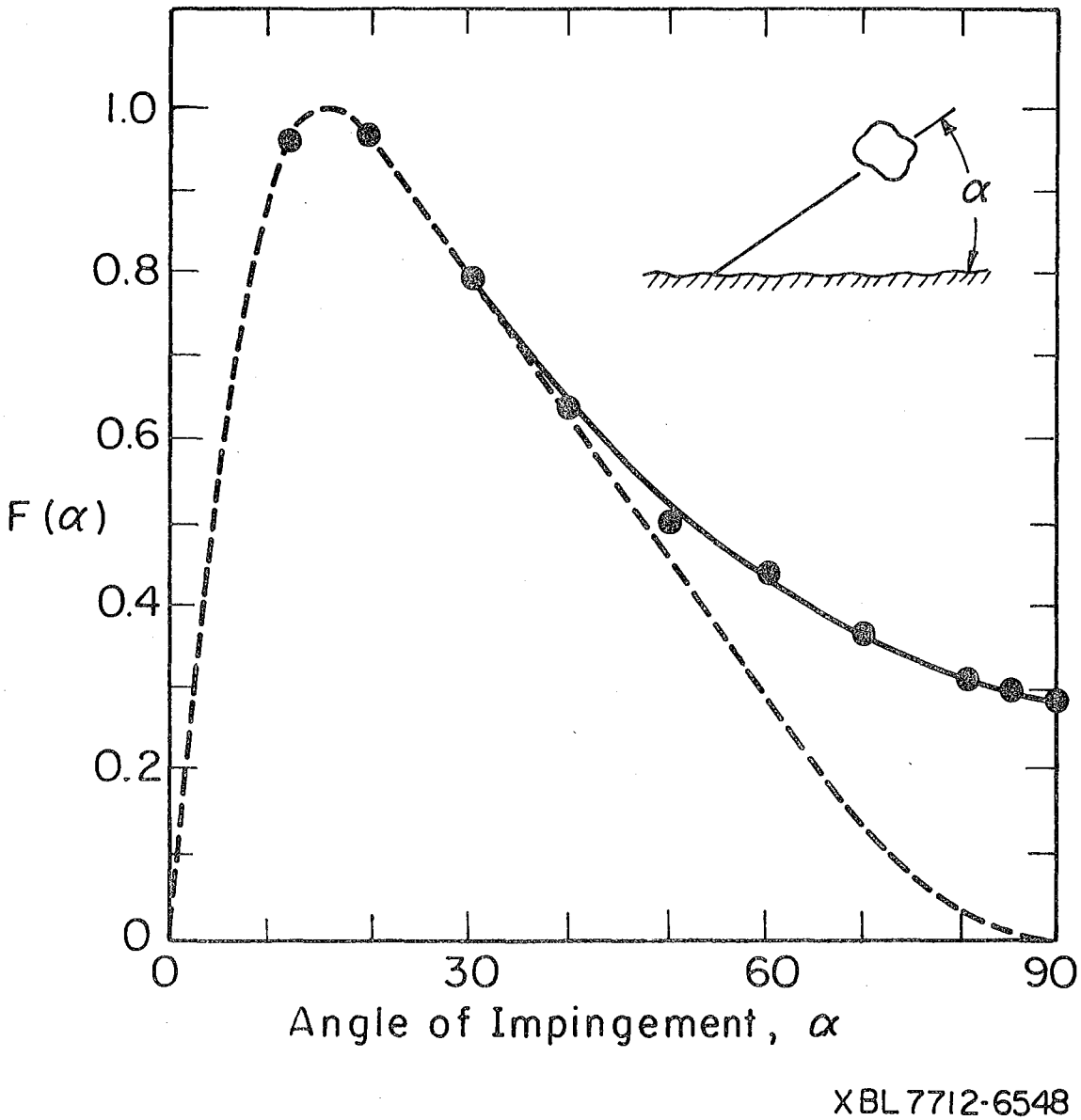

FIG. 5. General form of mass removal vs impingement angle for ductile erosion. Data points are for erosion of 1100-0 aluminum. Erosion curve was used to calculate relative erosion rate.

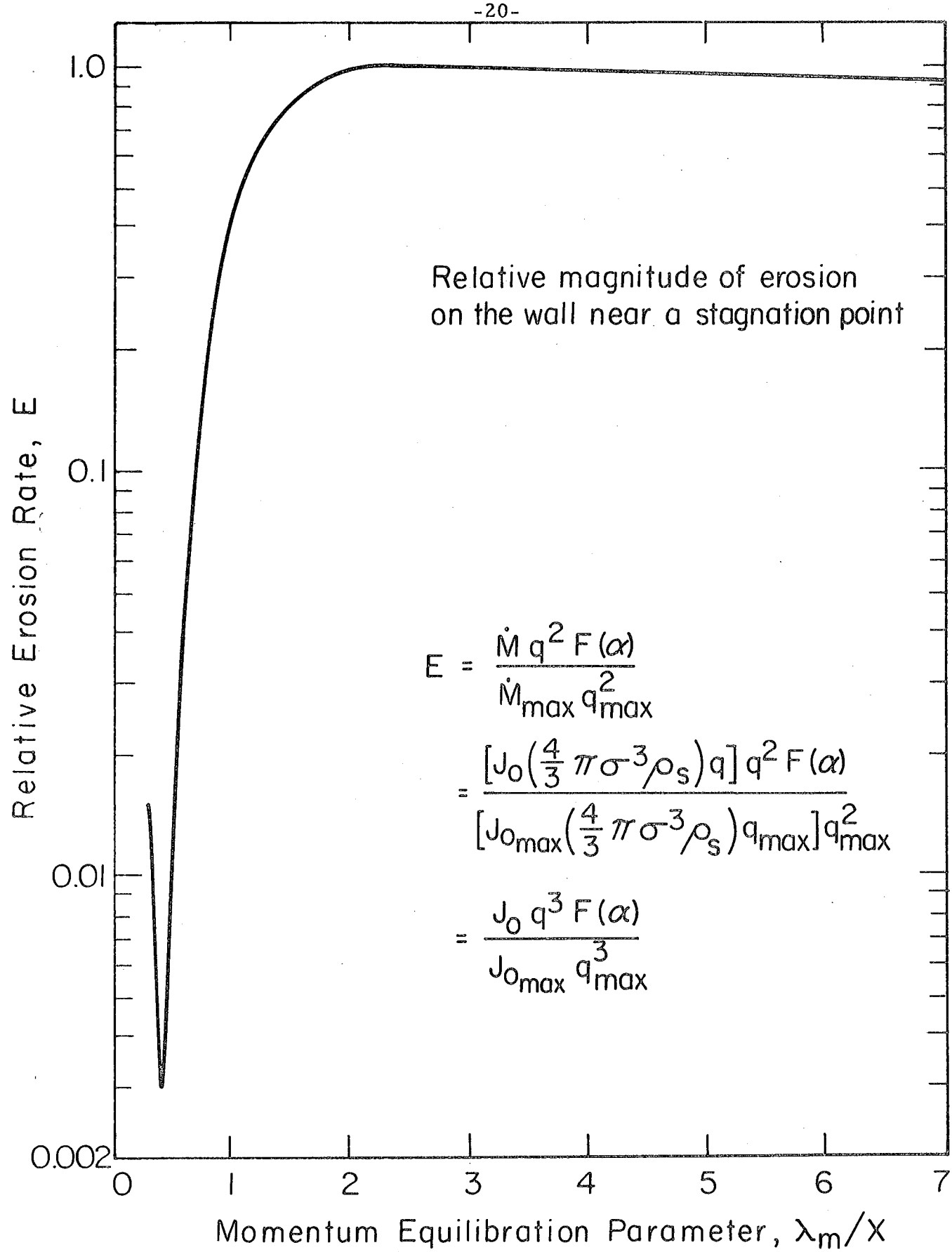

FIG. 6. Effect of momentum equilibration parameter on erosion. Since $E \sim q^3$ the curve exhibits characteristics predominated by the impact speed curve.

XBL 7712-6549

two relatively large components.

Now for λ'_m decreasing from 2 to 0.4, the particles experience a large deceleration in the x direction due to the increasing effect of the gas viscosity, leading to a small u velocity component and very low erosion levels.

This trend is suddenly reversed as λ'_m decreases further toward 0.25. Here the particles are entrained in the continuous phase over a long time interval, and consequently are accelerated with the continuous phase in the y direction. The impacts occur far from the stagnation point with the large v velocity component dominating the impact speed, and giving rise to the increased relative erosion rate. As noted previously, if $\lambda'_m \leqslant \frac{1}{4}$ the particles will not impact.

The minimum and maximum erosion points and respective values of the momentum equilibration parameter (namely 0.4 and 2.3) determine the physical particle characteristics that are desirable (or detrimental) in an operating two-phase system, depending on whether erosion is to be minimized (wear reduction) or maximized (abrasion).

D. Erosion pattern on wall

As an example, calculations are included for the particle sizes and velocities typical of a coal gasifier environment. In Eqs. (26) through (29), we take $\gamma = 10$ and $\beta = 0.1n$, $n = 0, 1 \ldots 10$. In this way the effect of a spatial distribution of like particles is examined to observe how erosion varies along the wall for a given initial velocity (see Figs. 7 and 8).

The previously described phenomenon of particle entrainment in

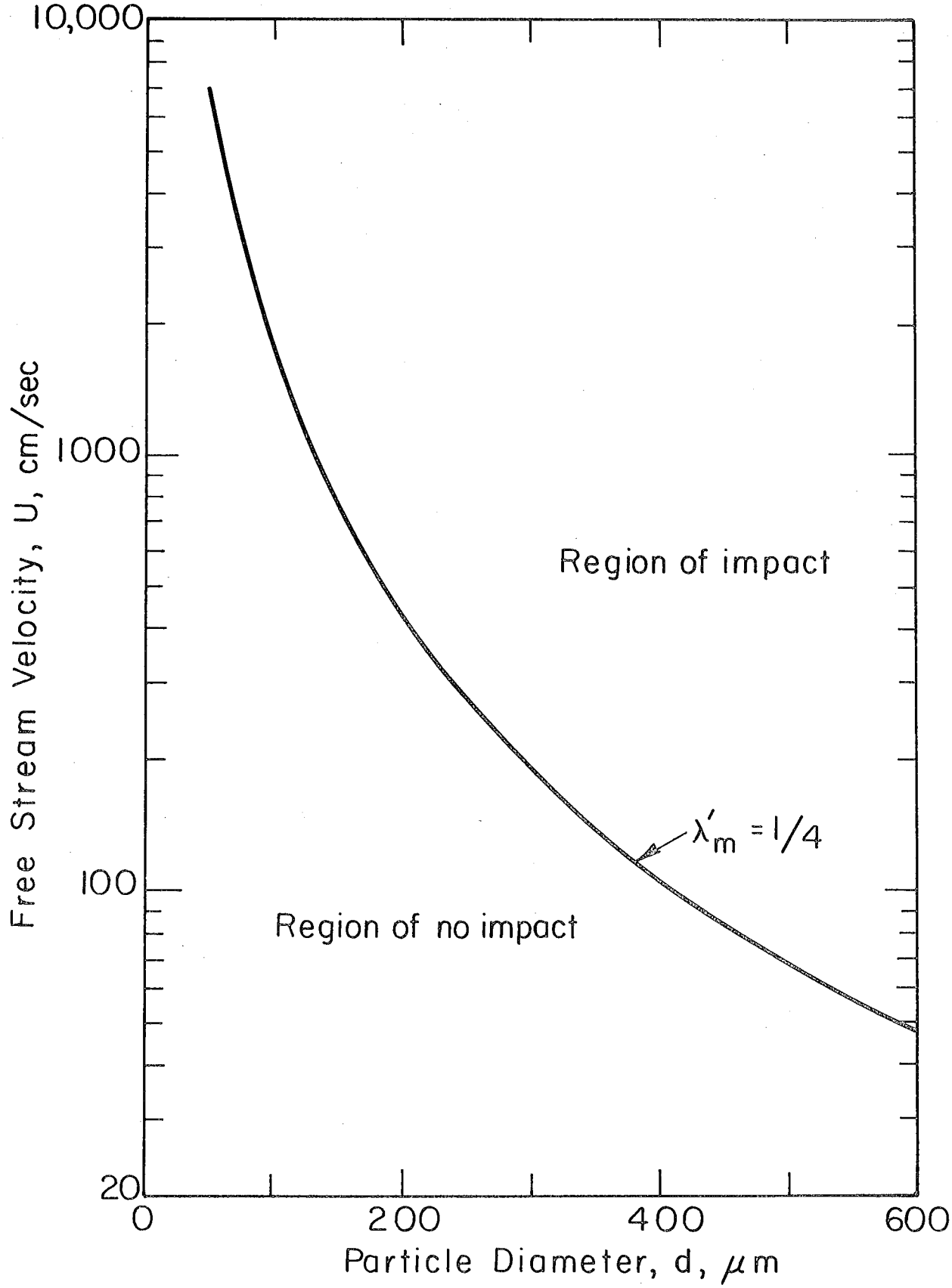

FIG. 7. Impact region. The curve indicates particles with a diameter and velocity such that they will not impact with the wall. The environment is typical of coal gasification systems.

XBL 7712-6550

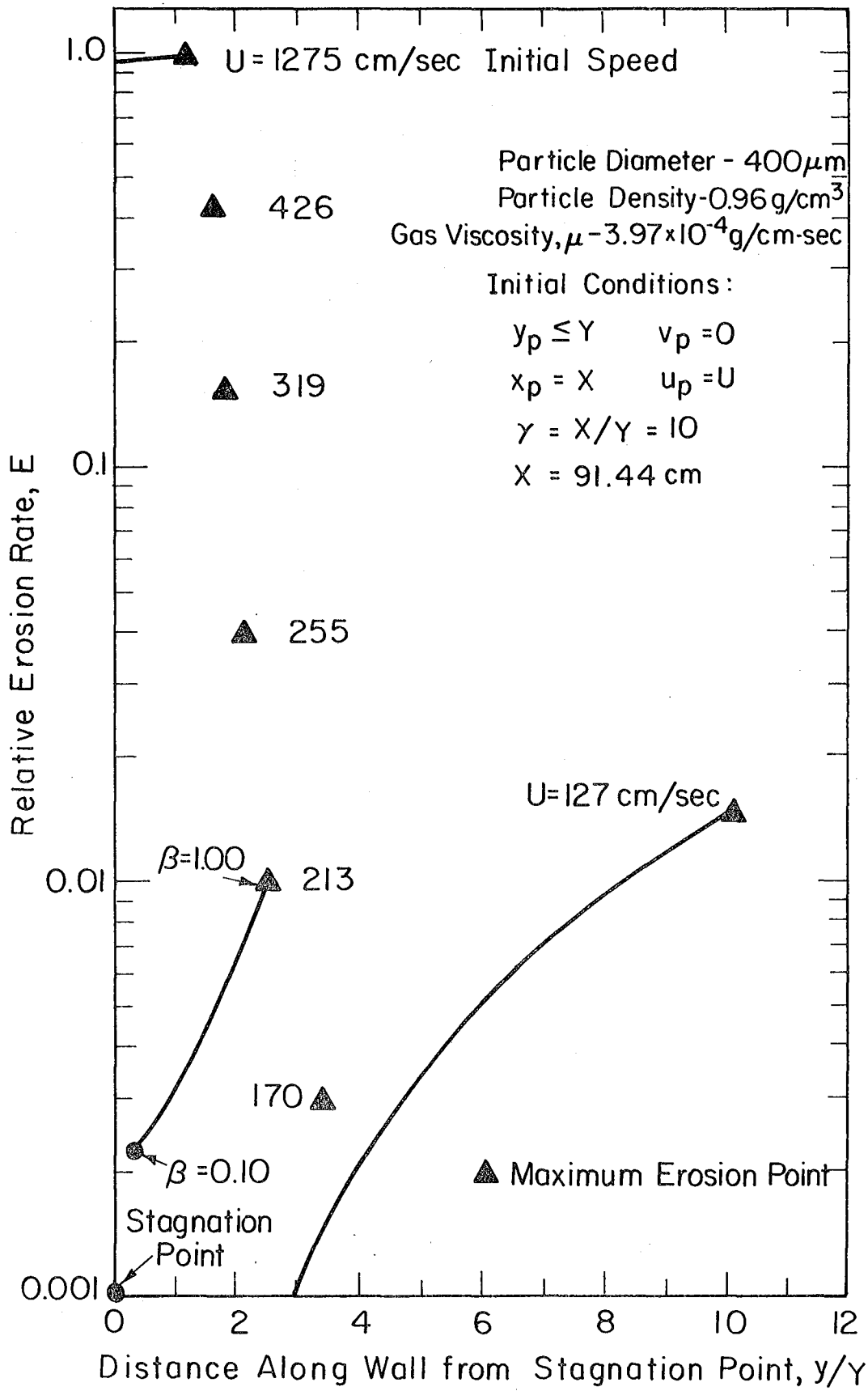

FIG. 8. Erosion pattern along the wall. The curves indicate the predicted magnitude of material removal for positions along the wall. The curves are erosion segments that correspond to particles starting initially at $X = 10Y$ and between $0 < y/Y \leq 1$.

XBL 7712-6551

the continuous phase and subsequent acceleration is clearly identifiable in the erosion pattern for 400μm particles. The maximum erosion for a particle with an initial speed of 127 cm/sec is somewhat higher than that for particles with 170 cm/sec and even 213 cm/sec, because the slower particles are entrained and accelerated away from the stagnation point. The corresponding erosion points are at a substantial distance from the stagnation point. Evidently, the maximum erosion for high-speed particles exceeds that for the slower particles by a factor of 100, and the distribution is nearly linear around the stagnation point.

The effect of the initial particle velocity on the erosion rate is illustrated in Fig. 9. Intuitively, this is expected to be proportional to the square of the velocity. However, the results show that the velocity exponent is normally greater than two. Sheldon and Kanhere[6] predicted velocity exponents as high as three. Grant and Tabakoff[3] found exponent values experimentally of the order of 4 in their work with turbomachinery.

The mean exponent value found in Fig. 9 is 3.83, with the value attaining a maximum of 7.70 in the regime corresponding to λ'_m equal to 0.5 .

Viscous effects near the wall should not influence these high exponent values of the velocity since they correspond to particles with large impact angles. Since the boundary layer is thin [i.e., $x/X = 0(10^{-3})$], only particles with very small impact angles will be slowed by the gas as it comes to rest at the wall.

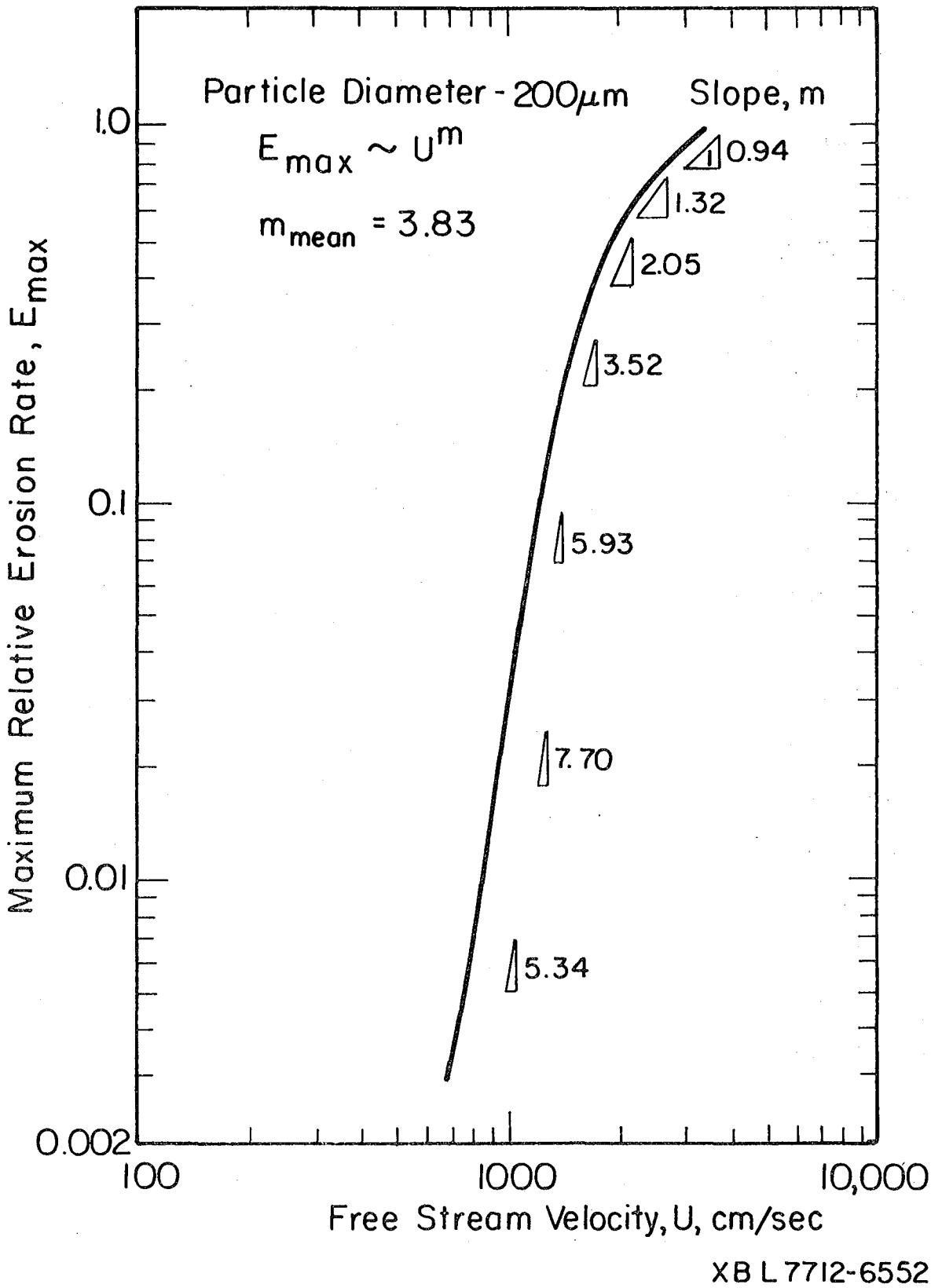

FIG. 9. Effect of free stream speed on erosion rate.

4. CONCLUSIONS

An analytical model is developed to predict erosion occurring near a stagnation point flow. The model takes account of the aerodynamic drag on the particles, the impact angle speed, and density, and determines the material removal along the wall. The solution is of a closed form type and is based on analysis of a single particle. The solution is readily applicable to a distribution of any number of like particles. However, when the number of particles becomes very large the continuous phase is altered and the assumption of continuous phase invariance under particle flows becomes invalid.

The momentum equilibration parameter is found to be the unique criterion for predicting particle trajectories. A cutoff value of $\lambda'_m \leqslant 0.25$ identifies those particles that never impact. The investigation shows that maximum erosion occurs for the value $\lambda'_m = 2.3$. The erosion is found to be proportional to the velocity raised to the mean exponent of 3.83.

To extend the present work boundary layer effects should be incorporated in the analysis of the stagnation point flow. Also the model would have wider application if particle-particle interactions and rebound phenomena were taken into account.

ACKNOWLEDGMENTS

The author wishes to express his sincere appreciation to Dr. Maurice Holt for his invaluable guidance and advice given freely throughout the course of this research.

This work was supported by the Division of Basic Energy Sciences of the Department of Energy.

[1] G.I. Taylor, "Notes on Possible Equipment and Technique for Experiments on Icing on Aircraft," Aeronautical Research Committee Reports and Memoranda, No. 2024, pp. 1-7 (1940).

[2] D.A. Drew, Arch. Ration. Mech. Anal. 62, No. 2, pp. 149-163 (1976).

[3] G. Grant and W. Tabakoff, J. Aircr. 12, No. 5, pp. 471-478 (1975).

[4] I. Finnie, Wear 19, pp. 81-90 (1972).

[5] G.L. Sheldon and I. Finnie, Trans. Am. Soc. Mech. Eng. 88B, pp. 387-392 (1966).

[6] G. L. Sheldon and A. Kanhere, Wear 21, pp. 195-209 (1972).

This report was done with support from the United States Energy Research and Development Administration. Any conclusions or opinions expressed in this report represent solely those of the author(s) and not necessarily those of The Regents of the University of California, the Lawrence Berkeley Laboratory or the United States Energy Research and Development Administration.

0 0 0 0 4 5 0 2 2 9 4